Robust Chemoenzymatic Synthesis of the Keratinimicin Aglycone Facilitated by the Structure and Selectivity of OxyB

Nicole Hauser,[1] Kendra A. Ireland,[2] Vasiliki T. Chioti,[1] Katherine M. Davis,[2,*] and Mohammad R. Seyedsayamdost[1,3,*]

[1]Department of Chemistry, Princeton University, Princeton, NJ 08544

[2]Department of Chemistry, Emory University, Atlanta, GA 30322

[3]Department of Molecular Biology, Princeton University, Princeton, NJ 08544

*Correspondence: kmdavis@emory.edu; mrseyed@princeton.edu

Abstract

The emergence of multidrug-resistant pathogens poses a threat to public health and requires new antimicrobial agents. As the archetypal glycopeptide antibiotic (GPA) used against drug-resistant Gram-positive pathogens, vancomycin provides a promising starting point. Peripheral alterations to the vancomycin scaffold have enabled the development of new GPAs. However, modifying the core remains challenging due to the size and complexity of this compound family. The recent successful chemoenzymatic synthesis of vancomycin suggests that such an approach can be broadly applied. Herein, we describe the expansion of chemoenzymatic strategies to encompass type II GPAs bearing all aromatic amino acids through the production of the aglycone analogue of keratinimicin A, a GPA that is five-fold more potent than vancomycin against *Clostridioides difficile*. In the course of these studies, we found that the cytochrome P450 enzyme $OxyB_{ker}$ boasts both broad substrate tolerance and remarkable selectivity in the formation of the first aryl ether crosslink on the linear peptide precursors. The X-ray crystal structure of $OxyB_{ker}$, determined to 2.8 Å, points to structural features that may contribute to these properties. Our results set the stage for using $OxyB_{ker}$ broadly as a biocatalyst toward the chemoenzymatic synthesis of diverse GPA analogues.

Main Text

The glycopeptide antibiotic (GPA) vancomycin (**1**, Fig. 1A) has long been used as a drug-of-last-resort against methicillin-resistant *Staphylococcus aureus* and *Clostridioides difficile*. It inhibits microbial growth by forming a supramolecular complex with the D-Ala-D-Ala terminus of nascent peptidoglycan strands, thus preventing crosslinking during bacterial cell wall construction.[1-6] After decades of clinical use, pathogens have acquired a resistance gene cassette through horizontal gene transfer, which allows them to evade vancomycin treatment. Instead of D-Ala-D-Ala, vancomycin-resistant bacteria incorporate D-Ala-D-lactate into the peptidoglycan.[7] The introduction of the depsipeptide linkage results in a 1,000-fold reduction in the binding affinity of vancomycin, rendering the drug ineffective.[8] With the emergence of multidrug-resistant pathogens, the discovery and development of novel antibiotics has become a task of highest relevance.

We recently reported a new GPA, keratinimicin A (**2,** Fig. 1A), from *Amycolatopsis keratiniphila* after activation of its otherwise silent biosynthetic gene cluster (BGC).[9] Keratinimicin A is a type II GPA, as classified by Nicolaou and co-workers, with a peptide consisting solely of aromatic amino acids.[10] In contrast to **1**, **2** contains L-Phe and D-3-chloro-4-hydroxyphenylglycine in the peptide backbone and is glycosylated at both L-3,5-dihydroxyphenylglycine (Dpg) and L-β-hydroxytyrosine; its disaccharide consists of L-rhamnose-D-glucose instead of L-vancosamine-D-glucose. Keratinimicin A is 5-fold and 4-fold more potent than **1** at inhibiting the growth of *Clostridium difficile* and *Streptococcus pneumoniae*, respectively. Isothermal titration calorimetry studies show that **2** binds to D-Ala-D-Ala with similar affinity as **1**, suggesting that the two GPAs share an analogous mode of action.[11] Upon activation of the keratinimicin BGC, several GPAs with closely related structures are produced, which renders the isolation of **2** tedious and limits access to sufficient quantities for further bioactivity studies. The chemical synthesis of **1** has been accomplished,[12-15] but GPA total synthesis remains challenging. An alternative chemoenzymatic approach toward the vancomycin aglycone was recently demonstrated by Forneris *et al.*[16,17] Although the two aryl ether crosslinks have been investigated on non-natural type II-like GPAs,[18,19] the synthesis of this GPA class has not yet been accomplished. Herein, we report the first synthesis of a type II GPA, the keratinimicin A aglycone analogue, using a chemoenzymatic approach. During this process, we identified a new OxyB homologue that is uniquely suited for the chemoenzymatic synthesis of GPA analogues, as determined by biochemical studies and an X-ray crystal structure of the enzyme.

To construct the keratinimicin aglycone, we pursued a similar approach to that used previously for **1**, [16,17] wherein the 7mer peptide is generated by solid-phase peptide synthesis (SPPS), appended onto the phosphopantetheinyl arm of the ultimate peptidyl carrier protein/X-domain [$(PCP_7\text{-}X)_{ker}$], and the crosslinks then installed enzymatically using the cytochrome P450 enzymes $OxyB_{ker}$, $OxyA_{ker}$, and $OxyC_{ker}$. To do so, we generated pure $(PCP_7\text{-}X)_{ker}$, $OxyB_{ker}$, $OxyA_{ker}$, and $OxyC_{ker}$ through recombinant expression in *Escherichia coli* (Table S1). As anticipated, all P450s purified with varying ratios of bound heme cofactors (typically 50%, Fig. S1, S2). We then optimized methods for synthesizing the highly nonpolar 7mer precursor peptide with suitable amide coupling and deprotection conditions to preserve epimerization-prone 4-hydroxyphenylglycine residues (Hpg, see Methods) (Fig. 1B, Fig. S3).[20,21] Replacement of the

standard fluorenylmethyloxycarbonyl (Fmoc) protecting group with ditertbutyl dicarbonate (Boc) for the ultimate residue proved essential to complete the synthesis of the heptapeptide, presumably because the Fmoc group exacerbated aggregation of the highly nonpolar polymer. Racemic Dpg was used due to fast epimerization during SPPS and subsequent steps, even under mild conditions. At residues 2 and 6, tyrosines rather than β-hydroxytyrosines were used due to facile dehydration at the benzylic carbon during SPPS. Upon cleavage of the peptide from the resin, a two-step thioesterification protocol was employed to enzymatically transfer the heptapeptide to the *apo* $(PCP_7\text{-}X)_{ker}$ didomain (Fig. 1B).[16,17] One-pot treatment of this tethered substrate with $OxyB_{ker}$, $OxyA_{ker}$, and $OxyC_{ker}$ followed by analysis via HPLC-coupled high-resolution mass spectrometry (HR-MS) after cleavage from the PCP_7-X didomain with propylamine showed formation of the tricyclic keratinimicin aglycone (Fig. 1C, 1D). HR-MS analysis revealed the unmodified substrate and the three products of $OxyB_{ker}$, $OxyA_{ker}$, and $OxyC_{ker}$. The locations of the crosslinks for each product were verified by tandem HR-MS (HR-MS/MS), which demonstrated the expected fragments outside of the macrocycle (Table S2). Yields are difficult to determine and likely to underestimate enzymatic conversion, because the ionization of the peptide is diminished after each crosslink; with that caveat in mind, we determined conversions of 55%, 5%, and 7% for $OxyB_{ker}$, $OxyA_{ker}$, and $OxyC_{ker}$, respectively. These results constitute the first synthesis of a type II GPA scaffold, thus expanding the utility of chemoenzymatic synthesis with complex natural products.

Interestingly, $OxyB_{ker}$ exclusively afforded the expected monocyclic product containing the C-*O*-D aryl ether linkage, as confirmed by HR-MS/MS analysis. This result is in sharp contrast to previous observations with the vancomycin OxyB ($OxyB_{van}$), which generates several products with the same *m/z* in enzymatic assays.[22-25] In fact, the promiscuity of $OxyB_{van}$ has been exploited to access diverse monocyclic products containing non-native crosslinks on heptapeptides.[22] While the generation of diverse monocyclic peptides can be useful, it also lowers the yield of the tricyclic product, the ultimate target in chemoenzymatic synthesis of GPAs. For chemoenzymatic synthesis of GPA analogs, the ideal OxyB should be promiscuous with respect to the peptide sequence but selective in installing a C-*O*-D crosslink. To assess whether Oxy_{ker} meets these criteria, we evaluated its performance on the vancomycin heptapeptide bound to the $(PCP_7\text{-}X)_{van}$ didomain (Fig. 2A). The reaction yielded a remarkably clean transformation to the monocyclic product compared to that achieved by $OxyB_{van}$ (Fig. 2B). We then assessed the reaction of $OxyB_{com}$ and $OxyB_{kis}$ from the complestatin and kistamicin pathways, respectively, with the vancomycin precursor bound to $(PCP_7\text{-}X)_{van}$. In both cases, no native crosslink was formed and a low conversion to side products was observed (Fig. 2C). These findings highlight the utility of $OxyB_{ker}$ as a biocatalyst with high tolerance for non-native substrates and, at the same time, high selectivity for the native C-*O*-D crosslink.

Early investigations into vancomycin biosynthesis showed that $OxyB_{van}$ is catalytically active in the absence of the X-domain.[26-28] Accordingly, we set out to investigate if $OxyB_{ker}$ strictly requires the X-domain for function, as this may help explain its high degree of *in vitro* selectivity for the C-*O*-D crosslink. Initial attempts to isolate $(PCP_7)_{ker}$ by heterologous expression in *E. coli* were unsuccessful owing to low expression levels. An *N*-terminal GB1-tag,[29-31] however, significantly boosted expression and allowed us

to isolate sufficient material for enzymatic activity assays with $OxyB_{ker}$. Analogous to the above procedure, the keratinimicin heptapeptide was prepared by SPPS and enzymatically transferred to *apo* GB1-tagged $(PCP_7)_{ker}$. Upon reaction with $OxyB_{ker}$, less than 2% conversion was observed, as compared to ~70% conversion with the $(PCP_7\text{-}X)_{ker}$-bound substrate (Fig. 2D). Thus, unlike $OxyB_{van}$, $OxyB_{ker}$ requires the X-domain for efficient crosslinking *in vitro*. We hypothesized that the structure of $OxyB_{ker}$ may differ from that of $OxyB_{van}$ in a manner that requires the X-domain for peptide binding and reactivity. In this model, the X-domain allows for precise placement of the heptapeptide in the OxyB active site and exclusively allows for C-*O*-D crosslink formation. $OxyB_{van}$, by contrast, can bind the substrate peptide in the absence of the X-domain, which allows the PCP-linked peptide to sample multiple orientations, resulting in regioisomeric products.

To test this model, we undertook crystallographic characterization of $OxyB_{ker}$. Repeated attempts to crystallize as-isolated $OxyB_{ker}$ failed, and suitably diffracting crystals were obtained following methylation of solvent-accessible lysine sidechains using standard methods.[32] The structure was subsequently solved to 2.8 Å resolution (PDB accession code 8F91) via molecular replacement with the homologous cytochrome P450 StaH (PDB accession code 5EX6),[33] which is involved in the biosynthesis of the teicoplanin-like GPA A47934, as the replacement model (Table S3). Like other OxyB enzymes characterized to date,[31,33-35] $OxyB_{ker}$ is primarily comprised of alpha helices organized into a canonical P450 fold with the heme cofactor coordinated by Cys347 (Fig. 3A, S4A). A comparison of published structures reveals remarkable conservation of the active site (Fig. S4B) with only subtle structural differences of surface features, most notably in the first β-sheet region (β-1) and G-helix (Fig. 3A, S5).[34] The former protrudes outward in $OxyB_{ker}$, in stark contrast to other OxyB models. However, this deviation is unlikely to be physiologically relevant, as lattice contacts clearly influence the orientation of the divergent β-hairpin loop (residues 28-45) via the continuation of the β-sheet between crystallographic symmetry mates (Fig. S4C). This region is also distant from the PCP_7-X binding sites, and therefore not expected to participate directly in catalysis.

The G-helix, by contrast, sits at the interaction surface between OxyB and the X-domain, as demonstrated by earlier crystallographic studies of $OxyB_{tei}$ (PDB accession code 4TVF).[31,35] While binding to the X-domain was not thought to significantly influence the structure of $OxyB_{tei}$ (PDB accession code 4TX3),[35] careful reassessment of the co-crystal structure, with a focus on this structural element, reveals that the loop region linking the F and G helices becomes more ordered, substantially elongating the G-helix (Fig. 3B). Such a rearrangement is likely important for facilitating interaction with the PCP, as PCP-binding primarily occurs through hydrophobic interactions and shape complementarity with contacts that include the elongated G-helix (Fig. S5).[31,35] We were unable to obtain crystals of the $OxyB_{ker}$/X-domain complex; however, our data suggest that the *N*-terminus of the G-helix is unstructured in the absence of the X-domain (Fig. S5A). The resultant short G-helix in $OxyB_{tei}$ and $OxyB_{ker}$ likely disrupts the PCP_7 binding site, and this disorder may help explain the often-diminished reactivity of OxyB alone (~25% for $OxyB_{tei}$, and ~2% for $OxyB_{ker}$). By contrast, the G-helix in $OxyB_{van}$ is rigid and adopts an extended conformation even in the absence of the X-domain (Fig. 3C). This stability likely provides an intact binding face for the

PCP_7-linked substrate. $OxyB_{van}$ is therefore preorganized for PCP binding and consequently exhibits *in vitro* activity with just the PCP_7-domain (~90% conversion to product) or even the CoA-conjugated peptide substrate (~50% conversion).[27]

Aside from binding, previous studies of $OxyB_{tei}$ and StaH suggest that contact between the PCP_7- and X-domains is crucial for substrate positioning within the associated P450 active site (Fig. S6).[33,35] Furthermore, reorientation of the proteins following recruitment of the P450 by PCP_7-X is also believed to be important. Thus, although $OxyB_{van}$ can bind PCP_7-linked substrates, improper and heterogenous placement of the peptide substrate in the absence of the X-domain may contribute to the formation of its diverse monocyclic products. The requirement of the complete PCP_7-X didomain for reactivity in $OxyB_{ker}$, by contrast, ensures that the peptide is bound in a productive conformation for C-*O*-D crosslink formation. It should be noted that the G-helix of StaH is also well-structured, but this enzyme has yet to be examined with its native substrate *in vitro* to assess requirement of the X-domain. Moreover, advantageous lattice contacts, which also impact other regions of its structure, may contribute to the observed ordering of the G-helix in StaH. The G-helix model remains to be assessed with StaH and other OxyB enzymes.

In conclusion, we report the first synthesis of the keratinimicin A aglycone analogue using SPPS and biocatalysis of the native cytochrome P450 enzymes $OxyB_{ker}$, $OxyA_{ker}$, and $OxyC_{ker}$. In the course of our studies, we noticed that $OxyB_{ker}$ displays substrate promiscuity, yet is highly selective for its native reaction *in vitro*. The high degree of selectivity for the C-*O*-D crosslink *in vitro* is in sharp contrast with the reaction catalyzed by $OxyB_{van}$ in vancomycin biosynthesis. $OxyB_{ker}$ strictly depends on the X-domain for catalytic activity. Based on the catalytic and structural analysis of $OxyB_{ker}$ presented herein, we propose that the governing factor for a selective C-*O*-D crosslink formation is lack of background activity in the absence of the X-domain. The identification of $OxyB_{ker}$ as a biocatalyst with high substrate tolerance and selectivity for the C-*O*-D crosslink is expected to improve the chemoenzymatic syntheses of GPA analogues in search for novel antimicrobial compounds.

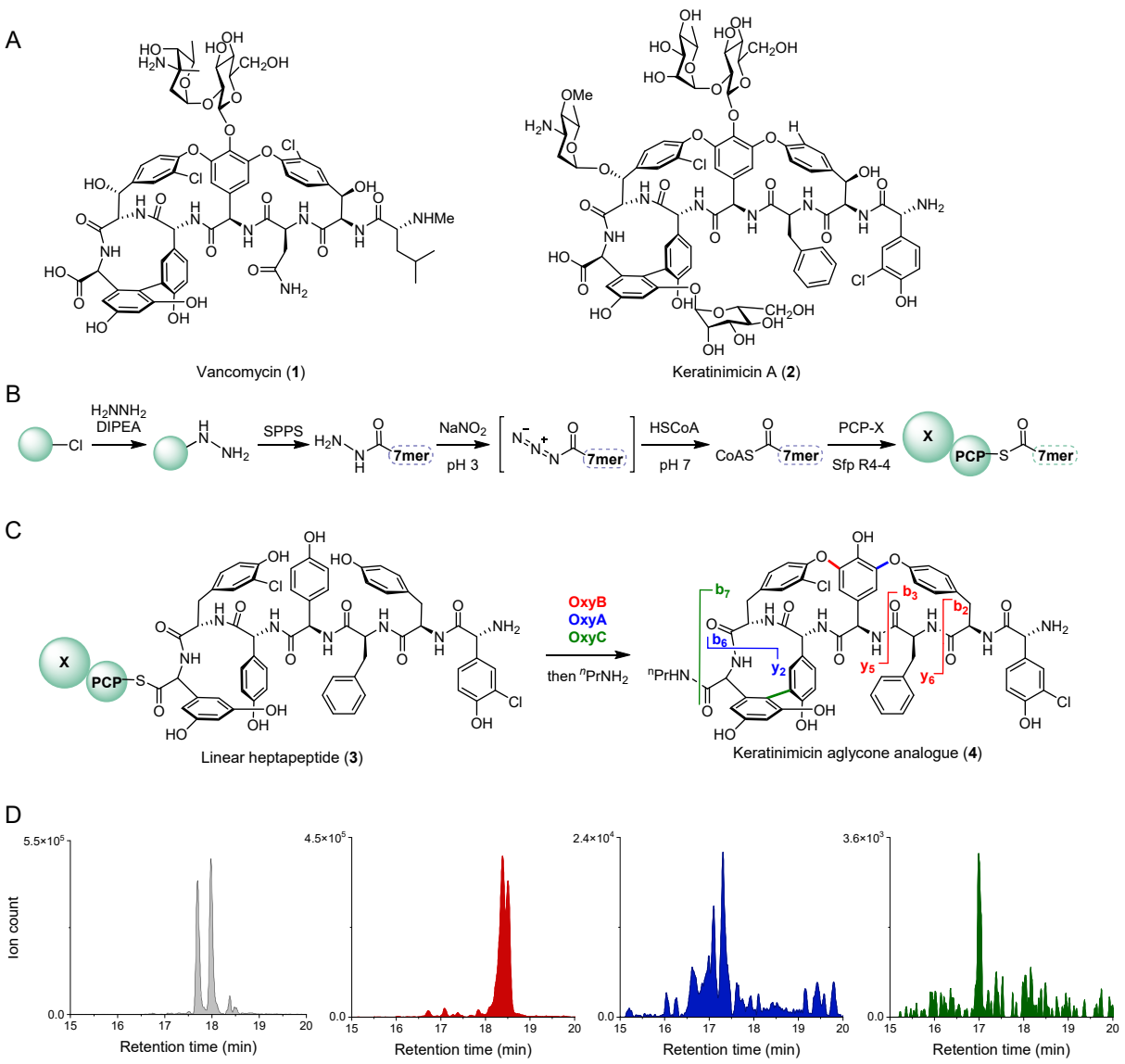

Figure 1. GPAs and the chemoenzymatic synthesis of the keratinimicin aglycone. (A) Structures of vancomycin (**1**) and keratinimicin A (**2**). (B) Synthetic scheme for the preparation of the 7mer-CoA precursor by SPPS followed by loading onto the PCP_7-X didomain using Sfp R4-4. (C) Treatment of the linear 7mer, conjugated to PCP_7-X, with $OxyB_{ker}$, $OxyA_{ker}$, and $OxyC_{ker}$ in one pot followed by release via propylamine leads to the formation of the aglycone analog, as characterized by HR-MS and HR-MS/MS. Observed HR-MS/MS fragments for mono-, bi-, and tri-cyclic products are shown and are color-coded. (D) Extracted ion chromatograms of starting material (grey), as well as the monocyclic (red), bicyclic (blue), and tricyclic (green) products.

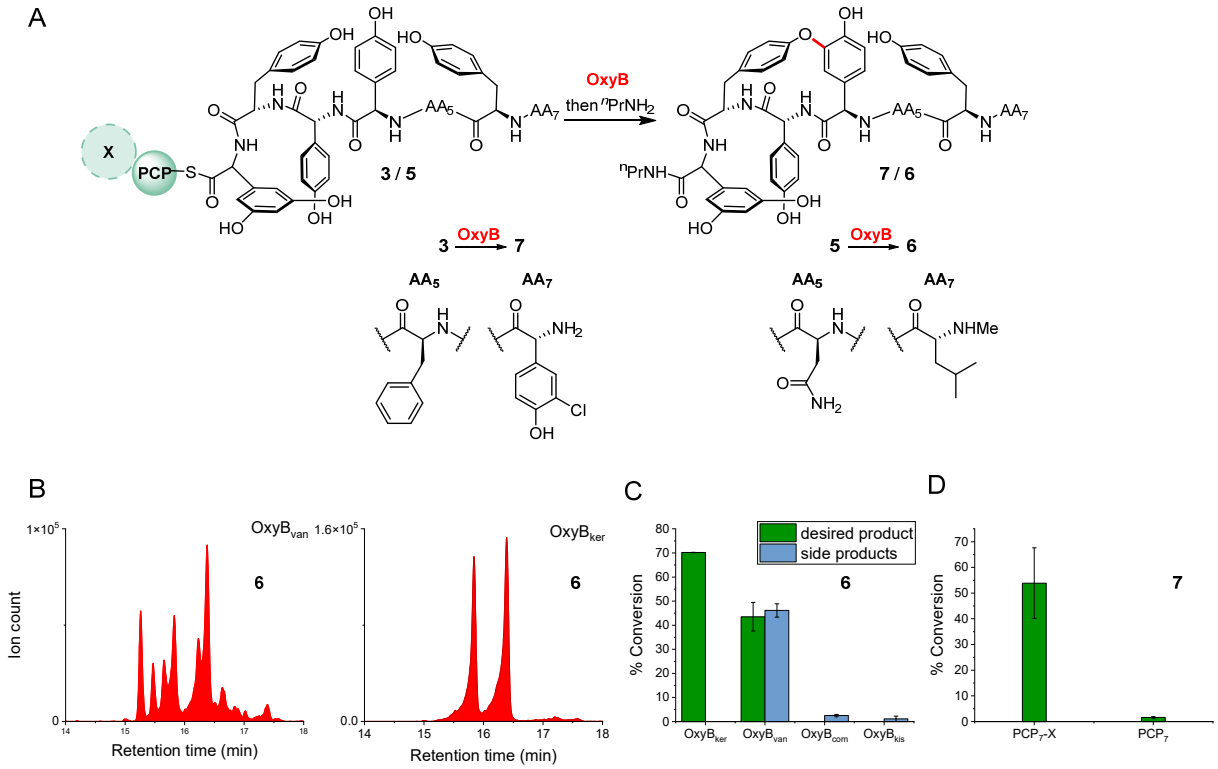

Figure 2. X-domain dependence of OxyBs. (A) Scheme for the monocyclization reaction for the keratinimicin A precursor (**3** -> **7**) or the vancomycin precursor (**5** -> **6**). (B) The monocyclization of vancomycin heptapeptide bound to $(PCP_7\text{-}X)_{van}$ by $OxyB_{ker}$ (right) is significantly cleaner than by $OxyB_{van}$ (left). (C) Comparison of catalytic activity of OxyB from the keratinimicin (ker), vancomycin (van), complestatin (com), and kistamicin (kis) biosynthesis with the vancomycin 7mer bound to $(PCP_7\text{-}X)_{van}$. (D) $OxyB_{ker}$ strictly requires the X-domain for converting its native heptamer analogue.

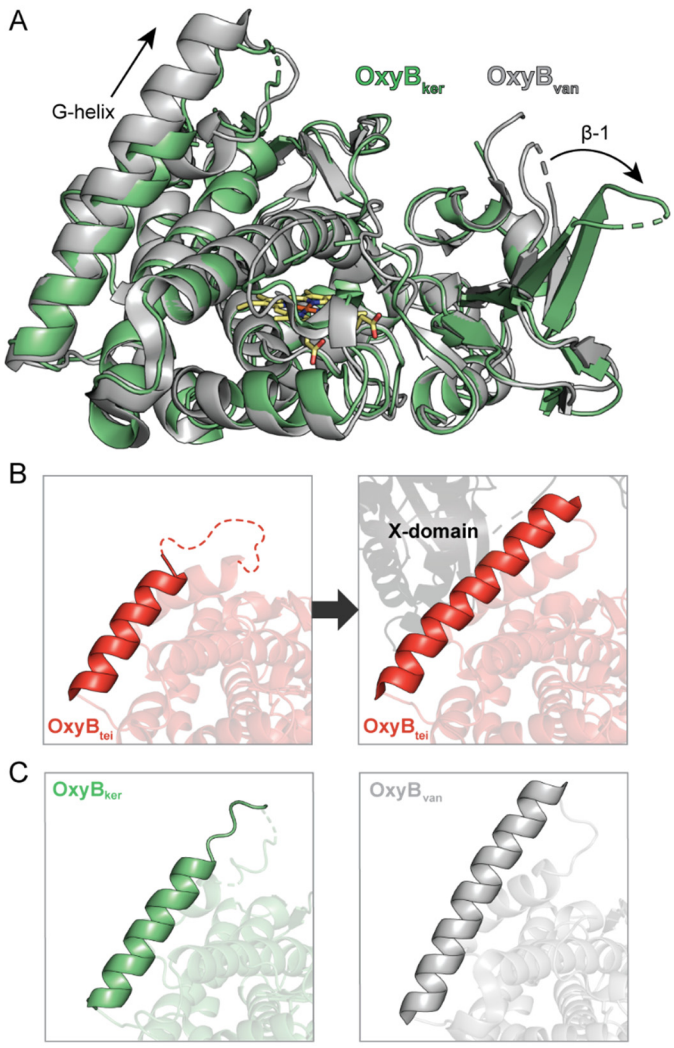

Figure 3. Crystal structure of $OxyB_{ker}$ and the importance of the G-helix. (A) X-ray crystal structure of $OxyB_{ker}$ (PDB accession code 8F91, green) overlaid with $OxyB_{van}$ (PDB accession code 1LFK, gray), with the heme cofactor shown in yellow. Main structural differences are found in peripheral loops (β-1) and the G-helix, which interacts with the X-domain in the teicoplanin system. (B) Elongation of the G-helix upon X-domain binding to $OxyB_{tei}$ (PDB accession code 4TVF [left] and 4TX3 [right]). (C) G-helix comparison of $OxyB_{ker}$ (left) with that of $OxyB_{van}$ (right); the latter is elongated in the absence of the X-domain.

Methods

Detailed protocols for cloning *oxyB*$_{ker}$, *oxyA*$_{ker}$, *oxyC*$_{ker}$, *oxyB*$_{van}$, *oxyB*$_{com}$, *oxyB*$_{kis}$ as well as (*pcp*$_7$-*x*)$_{ker}$, (*pcp*$_7$-*x*)$_{van}$ and *pcp*$_{7,ker}$, for synthesizing the CoA-heptapeptide, and for X-ray data collection and processing are provided in the SI.

General Procedures. UV–vis absorption spectra were acquired on a Cary 60 UV–visible spectrometer (Agilent). HPLC-HRMS and HR-tandem HPLC-MS were carried out on an Agilent 6546 accurate-mass quadrupole time-of-flight (Qtof) MS instrument, equipped with an automated liquid sampler, a 1260 Infinity II Series LC system, a diode array detector, a JetStream ESI source and the 6546 Series Qtof. Compounds were separated on an Aeris 3.6 µm PEPTIDE XB-C18 100 Å LC column (100 × 4.6 mm), operating at 0.5 mL/min with a gradient of 10% MeCN in H_2O to 50% MeCN over 20 min; all solvents contained 0.1% FA. Fast protein liquid chromatography (FPLC) was performed on a Bio-Rad NGC Chromatography System using a HiPrep 16/60 Sephacryl S-200 HR column (60 cm × 16 mm, 50 µm avg. part. size) with a flow rate of 0.3 mL/min.

Purification of OxyB$_{ker}$, OxyA$_{ker}$, and OxyC$_{ker}$. Detailed procedures for cloning and expression of 6His-OxyB$_{ker}$, 6His-OxyA$_{ker}$, and 6His-OxyC$_{ker}$ are provided in the SI. Enzyme purification was carried as previously reported, with slight differences in buffer compositions (see SI).[10a] Typical yields were 23 mg/L culture for 6His-OxyB$_{ker}$, 89 mg/L culture of 6His-OxyA$_{ker}$, and 94 mg/L culture of 6His-OxyC$_{ker}$.

OxyB$_{ker}$/OxyA$_{ker}$/OxyC$_{ker}$ assay. The enzymatic assay was based on previously described protocols.[7, 10] Reaction buffer (50 mM HEPES, 20 mM KCl, 10 mM $MgCl_2$, pH 7.0) was added to an Eppendorf tube containing 20 nmol of lyophilized peptide-CoA adduct, to a final concentration of 400 µM. Subsequently, final concentrations of 400 µM PCP$_7$-X and 80 µM of Sfp R4-4 were added and the mixture incubated at room temperature for 1.5 h. The following were sequentially added: reaction buffer to a total volume of 100 µL, 4 mM glucose-6-phosphate, 4 units of glucose-6-phosphate dehydrogenase, 21 µM *E. coli* flavodoxin reductase, 9 µM spinach ferredoxin, 7.5 µM OxyB$_{ker}$, 10 µM OxyA$_{ker}$, 12.5 µM OxyA$_{ker}$, and 4 mM NADPH. The mixture was incubated at room temperature for 3-4 h in the dark. In order to cleave the peptide from the carrier domain, 8 µL $^nPrNH_2$ were added, followed by incubation at room temperature for 15 min. Proteins were precipitated by adding 15 µL of formic acid and 50 µL of MeCN+0.1% FA. Centrifugation was followed by HR-HPLC-MS and MS/MS analysis of the supernatant.

OxyB$_{van}$, OxyB$_{com}$, OxyB$_{ker}$, and OxyB$_{kis}$ with (PCP$_7$-X)$_{van}$ assays. The loading reaction was performed as described above using 80 nmol of CoA-vancomycin analogue heptapeptide. The material was then split into 8 batches of 10 nmol (PCP$_7$-X)$_{van}$-loaded vancomycin heptapeptide. Assays were performed in duplicates with a total volume of 50 µL reaction buffer, 4 mM glucose-6-phosphate, 4 units of glucose-6-phosphate dehydrogenase, 20 µM spinach ferredoxin, 8 µM *E. coli* flavodoxin reductase, 20 nM of the respective OxyB, and 4 mM NADPH. The mixture was incubated for 1.5 h at room temperature in the dark. Work up and analysis were done as described above.

OxyB$_{ker}$ with (PCP$_7$-X)$_{ker}$ and PCP$_{7,ker}$ assays. Assays were performed in duplicate and as with the OxyB variants, except that the loading reactions were done separately on two 10 nmol batches.

OxyB$_{ker}$ crystallization. OxyB$_{ker}$ was purified over an FPLC column equilibrated with storage buffer (50 mM HEPES, 100 mM KCl, 10% glycerol, pH 7). Lysine methylation was performed at 4 °C. To a 6 mg/mL sample of OxyB$_{ker}$ in storage buffer, 20 µL of freshly prepared 1 M dimethylamine-borane complex (ABC) and 40 µL of 1 M methanol-free formaldehyde were added per mL of protein solution. The solution was gently mixed, then incubated for 2 h. The previous step was repeated, followed by addition of another 10 µL of 1 M ABC per mL of protein solution. After overnight incubation, 5 mg/mL glycine and 5 mM DTT were added. The mixture was incubated for another 2 h then concentrated to 20 mg mL^{-1}, determined

using the predicted 280 nm extinction coefficient of 33,920 M^{-1} cm^{-1}. Crystals were grown by sitting drop vapor diffusion at room temperature. 20 mg mL^{-1} $OxyB_{ker}$ in storage buffer was mixed 1:1 with a precipitant solution of 1.8 ammonium citrate tribasic pH 7. Red crystals appeared within three months. The crystals were looped and briefly transferred into cryoprotectant, comprised of the precipitant with 30% (v/v) ethylene glycol, before flash freezing in N_2(l).

Associated Content

Detailed description of materials and methods; UV-vis absorption spectra of Oxy enzymes; HR-MS and HR-MS/MS data for enzymatic assays; crystallographic and refinement statistics. These data are available free of charge at:

Acknowledgements

We thank the Swiss National Science Foundation Early "Postdoc Mobility" Fellowship (no. P2EZP2_187995 to N.H.), the National Science Foundation Graduate Research Fellowship Program (no. 1937971 to K.A.I.), the Edward C. Taylor 3rd Year Fellowship in Chemistry (to V.T.C.) and the National Institutes of Health (grant R35 GM147557 to K.M.D. and grant R01 GM129496 to M.R.S.) for financial support. This research used resources of the Advanced Photon Source, a U.S. Department of energy (DOE) Office of Science User Facility operated for the DOE Office of Science by Argonne National Laboratory under Contract No. DE-AC02-06CH11357. Use of the LS-CAT Sector 21 was supported by the Michigan Economic Development Corporation and the Michigan Technology Tri-Corridor (grant 085P1000817).

References

1. Perkins, H. R. Specificity of combination between mucopeptide precursors and vancomycin or ristocetin. *Biochem. J.* **1969**, *111*, 195-205.
2. Nieto, M.; H. R. Perkins, H. R. Modifications of the acyl-D-alanyl-D-alanine terminus affecting complex-formation with vancomycin. *Biochem. J.* **1971**, *123*, 789-803.
3. Williams, D. H.; Waltho, J. P. Molecular basis of the activity of antibiotics of the vancomycin group *Biochem. Pharmacol.* **1988**, *37*, 133-141.
4. Schäfer, M.; Schneider, T. R.; Sheldrick, G. M. Crystal structure of vancomycin *Structure* **1996**, *4*, 1509-1515.
5. Kahne, D.; Leimkuhler, C.; Lu, W.; Walsh, C. Glycopeptide and lipoglycopeptide antibiotics. *Chem. Rev.* **2005**, *125*, 425-448.
6. Williams, D. H.; Bardsley, B. The vancomycin group antibiotics and the fight against resistant bacteria. *Angew. Chem. Int. Ed. Engl.* **1999**, *38*, 1172-1193.
7. Walsh, C. T.; Fisher, S. L.; Park, I.-S.; Prahalad, M.; Wu, Z. Bacterial resistance to vancomycin: five genes and one missing hydrogen bond tell the story. *Chem. Biol.* **1996**, *3*, 21-28.
8. Bugg, T. D. H.; Wright, G. D.; Dutka-Malen, S.; Arthur, M.; Courvalin, P.; Walsh, C. T. Molecular basis for vancomycin resistance in *Enterococcus faecium* BM4147: Biosynthesis of a depsipeptide peptidoglycan precursor by vancomycin resistance proteins VanH and VanA. *Biochemistry* **1991**, *30*, 10408-10415.
9. Xu, F.; Wu, Y.; Zhang, C.; Davis, K. M.; Moon, K.; Bushin, L. B.; Seyedsayamdost, M. R. A genetics-free method for high-throughput discovery of cryptic microbial metabolites. *Nat. Chem. Biol.* **2019**, *15*, 161-168.
10. Nicolaou, K. C.; Boddy, C. N. C.; Bräse, S.; Winssinger, N. Chemistry, biology, and medicine of the glycopeptide antibiotics. *Angew. Chem. Int. Ed. Engl.* **1999**, *38*, 2096-2152.
11. Chioti, V. T.; McWhorter, K. L., Xu, F.; Jeffrey, J. D.; Davis, K. M.; Seyedsayamdost. M. R. Structural and functional analysis of keratinicyclin reveals synergistic antibiosis with vancomycin against *Clostridium difficile*. *ChemRxiv* **2021**. DOI: 10.26434/chemrxiv.14668545.v1.
12. Moore, M. J.; Qu, S.; Tan, C.; Cai, Y.; Mogi, Y.; Jamin Keith, D.; Boger, D. L. Next-Generation total synthesis of vancomycin. *J. Am. Chem. Soc.* **2020**, *142*, 16039-16050.

13. Boger, D. L.; Miyazaki, S.; Heon Kim, S.; Wu, J. H.; Castle, S. L.; Loiseleur, O.; Jin, Q. Total synthesis of the vancomycin aglycon. *J. Am. Chem. Soc.* **1999**, *121*, 10004-10011.
14. Nicolaou, K. C.; Mitchell, H. J.; Jain, N. F.; Winssinger, N.; Hughes, R.; Bando, T. Total synthesis of vancomycin. *Angew. Chem. Int. Ed. Engl.* **1999**, *38*, 240-244.
15. Evans, D. A.; Wood, M. R.; Trotter, B. W.; Richardson, T. I.; Barrow, J. C.; Katz, J. L. Total syntheses of vancomycin and eremomycin aglycons. *Angew. Chem. Int. Ed. Engl.* **1998**, *37*, 2700-2704.
16. Forneris, C. C.; Ozturk, S.; Gibson, M. I.; Sorensen, E. J.; Seyedsayamdost, M. R. In vitro reconstitution of OxyA enzymatic activity clarifies late steps in vancomycin biosynthesis. *ACS Chem. Biol.* **2017**, *12*, 2248-2253
17. Forneris, C. C.; Seyedsayamdost, M. R. In vitro reconstitution of OxyC activity enables total chemoenzymatic syntheses of vancomycin aglycone variants. *Angew. Chem. Int. Ed. Engl.* **2018**, *57*, 8048-8052.
18. Brieke, C.; Peschke, M.; Haslinger, K.; Cryle, M. J. Sequential in vitro cyclization by cytochrome P450 enzymes of glycopeptide antibiotic precursors bearing the X-Domain from nonribosomal peptide biosynthesis. *Angew. Chem. Int. Ed. Engl.* **2015**, *54*, 15715-15719.
19. Peschke, M.; Brieke, C.; Goode, R. J.; Schittenhelm, R. B.; Cryle, M. J. Chlorinated glycopeptide antibiotic peptide precursors improve cytochrome P450-catalyzed cyclization cascade efficiency. *Biochemistry* **2017**, *56*, 1239-1247.
20. Brieke, C.; Cryle, M. J. A facile Fmoc solid phase synthesis strategy to access epimerization-prone biosynthetic intermediates of glycopeptide antibiotics. *Org. Lett.* **2014**, *16*, 2454-2457.
21. Liang, C.; Behnam, M. A. M.; Sundermann, T. R.; Klein, C. D. Phenylglycine racemization in Fmoc-based solid-phase peptide synthesis: Stereochemical stability is achieved by choice of reaction conditions. *Tetrahedron Lett.* **2017**, *58*, 2325-2329.
22. Forneris, C. C.; Nguy, A. K. L.; Seyedsayamdost, M. R. Mapping and exploiting the promiscuity of OxyB toward the biocatalytic production of vancomycin aglycone variants. *ACS Catal.* **2020**, *10*, 9287-9298.
23. Ozturk, S.; Forneris, C. C.; Nguy, A. K. L.; Sorensen, E. J.; Seyedsayamdost, M. R. Modulating OxyB-catalyzed cross-coupling reactions in vancomycin biosynthesis by incorporation of diverse D-Tyr analogues. *J. Org. Chem.* **2018**, *83*, 7309-7317.
24. Forneris, C. C.; Ozturk, S.; Sorensen, E. J.; Seyedsayamdost, M. R. Installation of multiple aryl ether crosslinks onto non-native substrate peptides by the vancomycin OxyB. *Tetrahedron* **2018**, *74*, 3231-3237.
25. Tailhades, J.; Zhao, Y.; Schoppet, M.; Greule, A.; Goode, R. J. A.; Schittenhelm, R. B.; De Voss, J. J.; Cryle, M. J. Enzymatic cascade to evaluate the tricyclization of glycopeptide antibiotic precursor peptides as a prequel to biosynthetic redesign. *Org. Lett.* **2019**, *21*, 8635-8640.
26. Zerbe, K.; Woithe, K.; Li, D. B.; Vitali, F.; Bigler, L.; Robinson, J. A. An oxidative phenol coupling reaction catalyzed by oxyB, a cytochrome P450 from the vancomycin-producing microorganism. *Angew. Chem. Int. Ed. Engl.* **2004**, *43*, 6709-6713.
27. Woithe, K.; Geib, N.; Zerbe, K.; Li, D. B.; Heck, M.; Fournier-Rousset, S.; Meyer, O.; Vitali, F.; Matoba, N.; Abou-Hadeed, K.; Robinson, J. A. Oxidative phenol coupling reactions catalyzed by OxyB: A cytochrome P450 from the vancomycin producing organism. Implications for vancomycin biosynthesis. *J. Am. Chem. Soc.* **2007**, *129*, 6887-6895.
28. Geib, N.; Woithe, K.; Zerbe, K.; Li, D. B.; Robinson, J. A.. New insights into the first oxidative phenol coupling reaction during vancomycin biosynthesis. *Bioorg. Med. Chem. Lett.* **2008**, *18*, 3081-3084.
29. Gronenborn, A. M.; Filpula, D. R.; Essig, N. Z.; Achari, A.; Whitlow, M.; Wingfield, P. T.; Clore, G. M. A novel, highly stable fold of the immunoglobulin binding domain of streptococcal protein G. *Science* **1991**, *253*, 657-661.
30. Kim, J.-M.; Kim, Y.-S.; Kim, Y.-R.; Choi, M.-J.; DasSarma, P.; DasSarma, S. Bioengineering of *Halobacterium* sp. NRC-1 gas vesicle nanoparticles with GvpC fusion protein produced in *E. coli. Appl. Microbiol. Biotechnol.* **2022**, *106*, 2043-2052.
31. Haslinger, K.; Maximowitsch, E.; Brieke, C.; Koch, A.; Cryle, M. J. Cytochrome P450 $OxyB_{tei}$ catalyzes the first phenolic coupling step in teicoplanin biosynthesis. *ChemBioChem* **2014**, *15*, 2719-2728.
32. Kim, Y.; Quartey, P.; Li, H.; Volkart, L.; Hatzos, C.; Chang, C.; Nocek, B.; Cuff, M.; Osipiuk, J.; Tan, K.; Fan, Y.; Bigelow, L.; Maltseva, N.; Wu, R.; Borovilos, M.; Duggan, E.; Zhou, M.; Binkowski, T. A.; Zhang, R.; Joachimiak, A. Large-scale evaluation of protein reductive methylation for improving protein crystallization. *Nat. Methods* **2008**, *5*, 853-854.

33. Ulrich, V.; Peschke, M.; Brieke, C.; Cryle, M. J. More than just recruitment: the X-domain influences catalysis of the first phenolic coupling reaction in A47934 biosynthesis by cytochrome P450 StaH. *Mol. Biosyst.* **2016**, *12*, 2992-3004.
34. Zerbe, K.; Pylypenko, O.; Vitali, F.; Zhang, W.; Rouset, S.; Heck, M.; Vrijbloed, J. W.; Bischoff, D.; Bister, B.; Sussmuth, R. D.; Pelzer, S.; Wohlleben, W.; Robinson, J. A.; Schlichting, I. Crystal structure of OxyB, a cytochrome P450 implicated in an oxidative phenol coupling reaction during vancomycin biosynthesis. *J. Biol. Chem.* **2002**, *277*, 47476-47485.
35. Haslinger, K.; Peschke, M.; Brieke, C.; Maximowitsch, E.; Cryle, M. J. X-domain of peptide synthetases recruits oxygenases crucial for glycopeptide biosynthesis. *Nature* **2015**, *521*, 105-109.